

Effect on Flow and Pipe Structure Behaviours from Different Pressure and Pipe Thickness for Pipeline in UTHM Biodiesel Plant

Faris Syahmi Zulkifli¹, Zuliazura Mohd Salleh^{1*}

¹Department of Mechanical Engineering Technology, Faculty of Engineering Technology, University Tun Hussein Onn Malaysia 86400 Pagoh, Johor, MALAYSIA

*Corresponding Author Designation

DOI: <https://doi.org/10.30880/peat.2022.03.01.089>

Received 17 January 2022; Accepted 11 April 2022; Available online 25 June 2022

Abstract: A pipe is a tubular section or hollow cylinder, usually of circular cross-section, used to transport substances from one location to another, through which liquids, gases, and masses of small solids can flow. One of the places where piping systems are widely used are in plants. It is important to know what type of pipes are used in plants. Depending on the type of pipes, thickness, and the location of the pipe. In plants, piping is a system of pipes used to convey fluids such as liquids, slurry and gases from one location to another. This study involved the investigations of the velocity, pressure and stress distribution inside a pipeline located at UTHM Biodiesel power plant using three different pipe wall thicknesses which are 2.80 mm, 3.70 mm and 5.10 mm. The actual geometry of the pipe model was obtained from the actual geometry in the plant. There are two variables for pressure inlet used in this simulation which are 153 KPa and 250 KPa while the pressure outlet remains constant at 88 KPa. The results of the analysis were used to construct a risk indicator which predicts the risk in pipe wall performance. All pipe analysis was performed by using Fluid-Structure Interaction (FSI) method. The risk indicator was constructed with different pipe thicknesses in order to predict the risk that might happen to the lifespan of the pipe. The results show that the flow and structure behavior was affected by the thickness of the pipe and the highest risk occurred at the transition of fluid from a larger diameter to the smaller section of the pipe. The pipe with 5.1 mm wall thickness model records the highest outlet flow rate drop, pressure drop and maximum stress.

Keywords: FSI, Pipe Wall Thickness, Pressure Inlet

1. Introduction

Nowadays, one of the dominant components in the process infrastructure is the boundless network of pipelines. According to Rao [1], pipe is considered as the vein of any power plant as the transportation of fluid itself is a major task. In typical power plant industry, most of the fluids transported are hydrocarbons, water and steam at different temperatures and pressures. Piping systems are a critical part

*Corresponding author: zulia@uthm.edu.co

2022 UTHM Publisher. All rights reserved.

publisher.uthm.edu.my/periodicals/index.php/peat

of power plant construction because they have a significant influence on how efficiently and cost-effectively a plant operates [2]. Another important thing that in pipe is sizing, diameter and thickness, which are designated for pipe sizes. The system will achieve maximum efficiency by selecting the correct pipe size for the designed flow rate [3]. As the pipe diameter increased, the cost of the pipe increased while the pressure drops so that the liquid needs the least power [4]. The flow rate varies by length if the diameter is constantly maintained. The results are about half the amount of water at constant pressure through it per unit of time during twice the pipe length. The piping systems are also widely used at the power plant including Biodiesel plant [5].

In recent years, biodiesel has become one of the most commonly used biofuels to partially replace petroleum diesel fuel [6]. Due to its renewable, non-toxic, and environmentally friendly nature, biodiesel is an appropriate alternative solution for diesel engines. Table 1.1 shows the Technical properties of biodiesel [7] and renewable energy source and foundation are equal to all biodiesels. Biodiesel is also the first commercial diesel alternative to carburized to have a complete emission assessment. They are manufactured through the photosynthesis of solar energy into chemical energy and separated from early photosynthesis [5]. The term biodiesel is assigned to long-chain fatty acid monoalkyl esters produced from edible oils, non-edible oils, and waste oils produced through a trans esterification process triglycerides using methanol or catalyst [8].

Table 1: Shows The Technical Properties of Biodiesel [7]

Common name	Biodiesel (bio-diesel)
Common chemical name	Fatty acid (<i>m</i>)ethyl ester
Chemical formula range	$C_{14}-C_{24}$ methyl esters or $C_{15-25}H_{25-48}O_2$
Kinematic viscosity range (mm^2/s , at 313 K)	3.3 – 5.2
Density range kg/m^3 , at 288K)	860-894
Boiling point range (K)	>475
Flash point range (K)	420 – 450
Distillation range (K)	470 – 600
Vapor pressure ($mm Hg$)at 295K	>5
Solubility in water	Insoluble in water
Physical appearance	Light to dark yellow, clear liquid
Odor	Light musty/ soapy odor
Biodegradability	More biodegradable than petroleum diesel
reactivity	Stable, but avoid strong oxidizing agents

The outline of the pipe study is based at the UTHM Biodiesel Pilot Plant located in Batu Pahat, Johor is to study the effect on the flow and structure behaviours from different thickness and pressure inlet on the pipeline. From the study, it is needed very important urgency to be done in order to investigate what are the effect of change in pressure inlet and pipe thickness to the flow and structure of pipe itself, aside the pipeline.

2. Methodology

Fluid Fluent and Static Structural simulation methods were used in this study to represent the Fluid-structure Interaction (FSI). To simulate all cases in both simulations. The flow behaviour and stress distribution along the pipeline were investigated using Fluid Fluent and Static Structural. The pipe structure is sketched in SolidWorks with three different pipe wall thickness. By inputting two different values of inlet velocity, both simulation methods were analyzed. The velocity, pressure, and stress distribution affected by this variable inlet value were then tabulated and analyzed to determine pipeline prediction risk which located at the fitting of the pipe.

2.1 3D Modelling

The geometric pipeline model is taken pipeline and then were drawn using SolidWorks which consist a total of 11 parts. The piping model were constructed from the actual dimension measured at

first. Then two others pipe model were created by altering thickness of pipe based on standard of pipe that use in plant. Referring to the actual thickness of the piping which is 3.7mm , this thickness is taken from schedule 40 for stainless steel. The other two parameter for thickness will be one schedule upper and one schedule lower than the actual. Schedule 10 with thickness of 2.8 mm and schedule 80 with thickness of 5.1 mm were used in this simulation.

2.2 Grid Generation for Fluid and Structure Domain

Grid generation, also known as meshing, is an important step in the CFD simulation process because it influences not only simulation time but also the accuracy of the study's results. A mesh is a discrete number of points arranged to cover the entire domain geometry. The pursuit of a well-constructed mesh is as important as prescribing the necessary physics to the flow problem. As a result, grid generation, as it is commonly known within the CFD community, has evolved into its own entity and remains a very active area of research and development. Grid generation is an essential consideration in obtaining numerical solutions to the CFD problem's governing partial differential equations [9].

Although a very coarse and poor-quality mesh or grid can be solved on a very powerful solver, it frequently results in non-physical or highly inaccurate simulation results. As a result, the grid generation skills, capability, and exposure are just as important as the solver operations. In any CFD project, model setup, particularly grid generation, is critical for time, cost, and quality of results [10]. The lack of methods for generating a computational grid suitable for fast and reliable numerical analysis is a limiting factor for the use of advanced 3D CFD tools in the analysis and design of rotary vane machines [11]. The aspect of grid generation is an important numerical issue where the specific mesh for a given flow problem can determine the success or failure in obtaining a computational solution [9].

2.2.1 Grid Independence Test

The grid independence test was done firstly to ensure the simulation reliability. A grid independent test (GIT) was conducted to assess the optimal grid resolution range derived based on a previous study to exclude possible biases owing to subjective judgment in the selection of grid conditions. The analysis begins with a coarse mesh and it is refined to finer mesh for each run until the results do not change significantly and depend of the grid size anymore. As the grid or mesh size approaches zero, the approximate solution is almost equal to the actual solution [12].

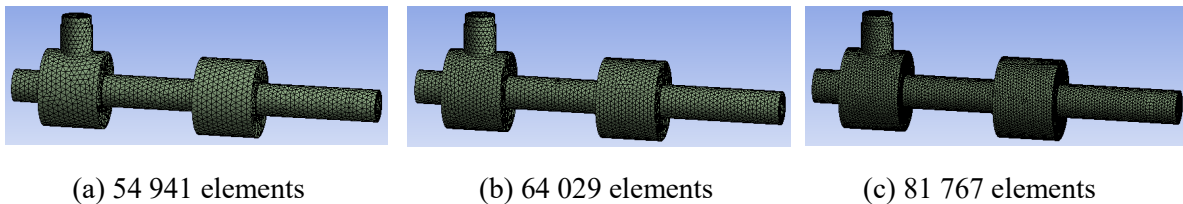


Figure 2: 3D Model of pipeline with 64029 number of meshing elements

Figure 2 depicts three different mesh refinement from the figure above. All the refinement has the different element which is Figure 2 (a) 81 767 elements, meanwhile Figure 2 (b) 64 029 elements and Figure 2 (c) 81 767 elements. The mesh with 64029 elements were chosen to use for run the simulation because the insignificant different between three numbers of elements. Figure 3 illustrate the grid independence test by evaluating the velocity along the centerline of the pipe model with different number of elements.

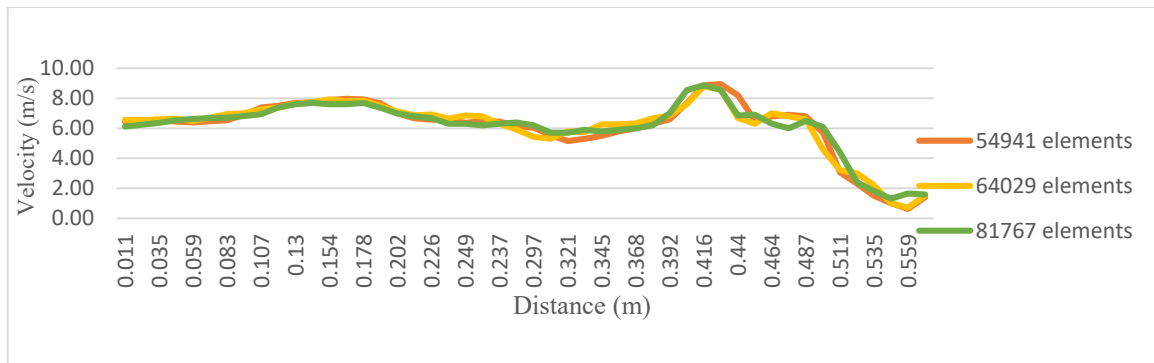


Figure 3: Velocity (m/s) VS Distance for 3 Different Element Numbers

2.3 Simulation Analysis

To analyzing all models used in this study, several software has been used. Ansys Fluent used to analyze the flow behavior effect from three different inlet pressure at Biodiesel plant. In addition, Ansys Mechanical will also be used together as one-way FSI method to study pipe wall performance effect by simulate the effect of different pressure inlet and pipe thickness.

2.3.1 Simulation for Fluid Flow

i. Navier-Stokes Equation

The Navier-Stokes equations are the guiding formulations for the flow, and the code available is based on a compressible formulation and solves the Reynolds-averaged Navier-Stokes equations (RANS). The basic RANS equation integrated over a control volume V , with an elemental surface area $d\vec{S}$, is expressed as in Eq. 1

$$\int_V \rho \frac{dU}{dt} dV + \int_S \vec{F} \cdot d\vec{S} = \int_S \vec{Q} \cdot d\vec{S} \quad Eq. 1$$

Where U is the conservative variable matrix containing density (ρ), the three components of mass flow ($\rho u, \rho v, \rho w$) and energy (ρE); and \vec{F} and \vec{Q} are the inviscid and viscous fluxes, respectively.

ii. Bernoulli Equation

The Bernoulli Equation, applied to moving fluids, is a particular way of conserving the energy theory. The pressure, the kinetic energy and the potential gravitational energy of a fluid in a vessel or flowing in a tube are related. The equation is written as in Eq. 2, where P is a static pressure head, v is a velocity of the fluid, ρ is a density of the fluid, h is a height of the container or the pipe here the fluid is flowing, g is a gravitational acceleration, $\frac{1}{2} \rho v^2$ is a velocity head and ρgh is a Hydrostatic pressure head.

$$P + \frac{1}{2} \rho v^2 + \rho gh = \text{constant} \quad Eq. 2$$

iii. Continuity Equation

The continuity equation shows that the product of the pipe's cross-sectional area and fluid velocity is always steady at every point across the path. This product is equal to the volume flow per second or simply the fluid velocity as shown in Eq. 3, where R is the volume flow rate, A is the flow area and v is the flow velocity.

$$R = A v = \text{constant} \quad Eq. 3$$

iv. Boundary Condition for Fluid

Summary on boundary condition parameters used in this CFD simulation were tabulated in Table 2.

Table 2: Parameter used in fluid analysis setting

Thickness (<i>mm</i>)	2.8 <i>mm</i>		3.7 <i>mm</i>		5.1 <i>mm</i>	
Inlet Pressure (KPa)	153	250	153	250	153	250
Outlet Pressure (KPa)	88					
Viscosity, μ (P)	$5.68e^{-3}$					
Density (Kg/m^3)	878					

2.3.2 Structure Analysis and Boundary Conditions

i. Young's Modulus

The Young's modulus (E), also known as elastic modulus, which defines the relationship between stress (σ) and strain (ϵ) in a linear elastic material, can be calculated using the following Eq. 4.

$$E = \sigma/\epsilon \quad Eq. 4$$

ii. Boundary Condition for Structure

Summary on all boundary condition parameters used in this CFD simulation study were tabulated in Table 3.

Table 3: Material properties for structural components (The European Stainless-Steel Development Association (Euro Inox), 2007)

Type of pipe	Young's Modulus E (N/mm^2)	Density (kg/m^2)	Poisson Ratio
Stainless Steel	$1.93e^{11}$	7750	0.31

3. Results and Discussion

The steady-state simulation results of flow behaviour velocity and pressure distribution were discussed and analyzed. The results are presented in the form of a contour plot, with each color representing a different magnitude of fluid flow. The magnitude of the flow can be used to predict its behaviour.

3.1 Velocity Distribution in Pipe

The Ansys Fluent software was used to analyse the flow behaviour in all the pipe model. The flow analysis was taken place to investigate the velocity and pressure distribution throughout the pipe. The centerline was plotted along the pipe. The results of the analysis were extracted from the centerline. Figure 4 depicts the velocity distribution in 2.80 mm, 3.70 mm, 5.10 mm with 153 KPa and 250 KPa pressure inlet. The maximum reading recorded at 153 Kpa (a) 6.80 m/s, (b) 9.7 m/s and (c) 12.50 m/s. The pressure drop in a laminar flow is proportional to the volumetric flow rate. When the flow rate is doubled, the pressure drop doubles. Pressure drop increases as the square of the volumetric flow rate in turbulent flow conditions. When the flow rate is doubled, the pressure drop increases fourfold. By reducing the diameter of the pipe, the flowing fluid can be compressed. It moves more quickly, resulting in a higher flow rate. Moreover, as the diameter increases, the flow rate decreases.

153KPa

250KPa

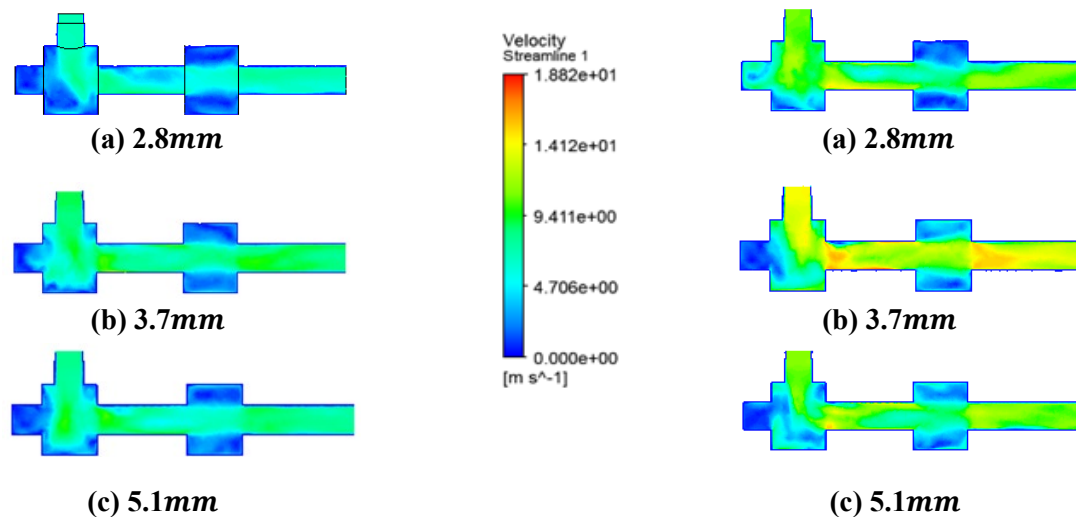


Figure 4: (a) 2.8mm, (b) 3.7mm and (c) 5.1mm Pipe Thickness with different Pressure Inlet

Figure 4 shows the velocity distribution contour results at 2.8 mm, 3.7 mm and 5.1 mm pipe wall thickness for 250 KPa, respectively. The results show a comparison of different velocity and thickness applications. The reading recorded for 250 KPa was (a) 8.7 m/s, (b) 11.6 m/s and (c) 14.1 m/s. Factors affecting water distribution uniformity can be divided into two groups which the first is directly related to the structure of the model, such as having pressure or non-pressure compensating. The second factor is related to the flowing characteristics in the lateral line, pressure loss along the pipe, clogging in partial or complete [13]. The pressure drop in a laminar flow is proportional to the volumetric flow rate. When the flow rate is doubled, the pressure drop is also doubled. Pressure drop increases as the square of the volumetric flow rate in turbulent flow conditions. When a fluid flows through a pipe, its momentum is transferred to the pipe wall, resulting in a force acting in the direction of fluid movement. This force is described as a frictional drag on the pipe wall's inside [14].

The results from this model was used to compare with others geometry of pipe. In pipe flow, gravity has no effect except for a hydrostatic pressure variation across the pipe that is usually negligible. It is the pressure difference, between one section of the horizontal pipe and another which forces the fluid through the pipe. In the entrance region of a pipe the fluid in the entrance region of a pipe, the fluid accelerates or decelerates as it flows. There is a balance between pressure, and inertia force [15].

3.2 Pressure Distribution in Pipe

Figure 5 depicts a comparison of the pressure distribution contour throughout the pipe at various pressures. Except at the inlet, there are no significant pressure differences for the model. The fluid entering the pipe at different pressures creates a slightly change in color contour at the bottom section before entering the other part. As the pressure at the inlet decreases, the pressure at the outlet remains constant. Inside the pipe, the maximum pressure recorded for 153.0 KPa was (a) 135.4 KPa, (b) 138.8 KPa, and (c) 139.7 KPa. The contour view of pressure distribution in 250.0 KPa shown in Figure 5. The pressure distribution results were compared using different pipe thickness with (a) 215.7 KPa, (b) 218.6 KPa and (c) 231.6 KPa. The contour depicts the colour difference at the bottom of the pipe inlet, where the water first hits the bottom section, creating turbulent flow before entering the smaller section of the pipe. The pressure distribution begins to remain constant as it approaches the outlet. The pressure distribution was high at the inlet before switching to the other section, resulting in a steady flow. While increasing pipe wall thickness does not increase standing fluid pressure, it does reduce resistance to pressure drop in flowing fluid. There is some pressure drop along the pipe when flow is in a narrow pipe. The pressure drop per foot of pipe is reduced when a larger diameter pipe is used. All of the results obtained show a nearly identical trend. It can be concluded that the greater the thickness of the pipe

wall, the greater the pipe's ability to withstand pressure. The pipe's thickness is important depending on where it is laid and what material passes through it [2].

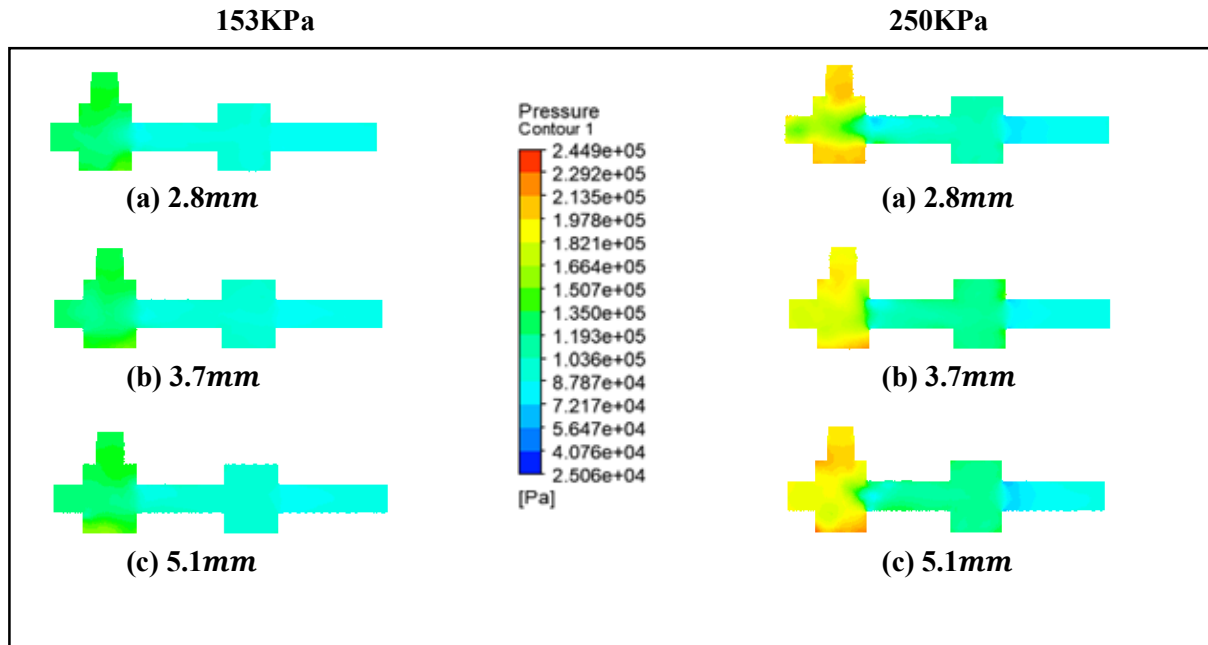


Figure 5: (a) 2.8mm, (b) 3.7mm and (c) 5.1mm Pipe Thickness with different Pressure Inlet

3.3 Stress Distribution in 153KPa Pressure Inlet

Pipe stress analysis is an analytical method to determine the piping system behaves based on its material, pressure, temperature, fluid, and support. Pipe stress analysis is a good approximation. It is important to understand the various types of pipe stresses, the process, and other items related to pipe stress analysis for best practices in performing a pipe stress analysis. Another reason a pipe stress analysis is performed is to increase the life of piping.

3.3.1 Stress Distribution in 153 KPa Pressure Inlet

Figure 6 depicts the stress distribution on the 153.0 KPa pressure inlet. The stress distribution recorded was (a) 9.7 MPa, (b) 8.5 MPa, and (c) 7.4 MPa. was even in the 153KPa pressure inlet. The highest stress distribution recorded in Figure 6 (a) was 8.5 MPa, while Figure 6 (b) recorded 13.4 MPa (b). Before entering the smaller section of the pipe, the stress distribution was significantly increased. The visible pipe wall deformation was observed in the 250 KPa pipe. Because of the high pressure of the fluid inside the pipe, the stress on the pipe wall increases.

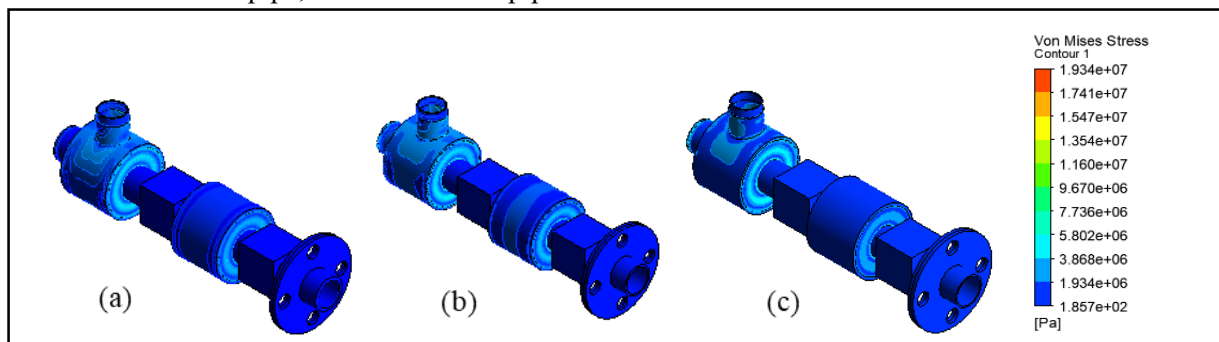


Figure 6: (a) 2.8mm, (b) 3.7mm and (c) 5.1mm Pipe Thickness with 153KPa Pressure Inlet

3.3.2 Stress Distribution in 250KPa Pressure Inlet

The stress distribution along the pipe wall was also predicted and presented in Figure 7. The maximum stress distribution recorded was (a) 14.8 MPa, (b) 13.3 MPa, and (c) 12.1 MPa. The contour

view shows the change pattern of stress distribution in due to the high pressure of the fluid. When a high-pressure fluid enters the inlet, it creates turbulent flow and collides with the pipe's wall. In the pipe wall, the stress distribution began to show an uneven distribution. The stress of pipe wall was higher before enter the smaller pipe section and decrease after that. It can be concluded that the higher the wall thickness, the lower stress distribution recorded. The thickness of the pipe is important depending on where it is laid and what material passes through it. The more flexible a pipe is, the fewer stresses it will experience due to the water hammer [16].

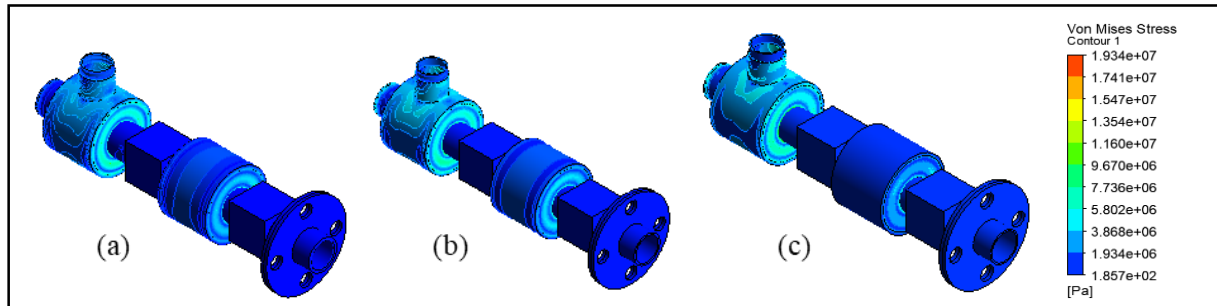
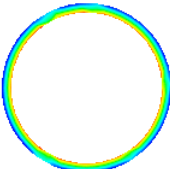
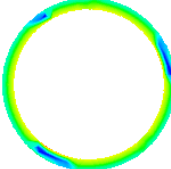
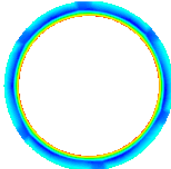
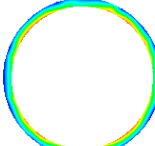


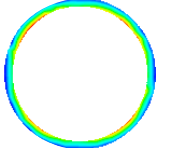
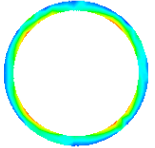



Figure 7: (a) 2.8mm, (b) 3.7mm and (c) 5.1mm Pipe Thickness with 153KPa Pressure Inlet

3.4 Risk Indicator

The risk indicator was constructed in order to estimate the risks of the different pressure inlet at different thickness of the pipe. The indicator was shown the cross section at the fitting throughout of the pipe as shown in Table 1 and Table 2. The main purpose of studying at each fittings location because it is a welded place to connect one parts to another parts, it is important to ensure that the connection is in good condition. If the reading of the stress distribution value on the connection is above normal, it can be said that the welding is not properly done or the installation incorrect and can cause major problem to the pipe. It will fail or worse it is likely that the pipe will leak due to high pressure.

Table 1: Stress Distribution Along the Fitting at 153 KPa Pressure Inlet

Risk	2.8mm	3.7mm	5.1mm
Fitting 1	 Min = 549.64KPa Max = 891.93KPa	 Min = 224.53KPa Max = 868.27KPa	 Min = 219.99KPa Max = 640.68KPa
Fitting 2	 Min = 395.08KPa Max = 663.54KPa	 Min = 308.14KPa Max = 533.50KPa	 Min = 258.29KPa Max = 444.20KPa
Fitting 3	 Min = 380.71KPa Max = 712.98KPa	 Min = 300.24KPa Max = 538.40KPa	 Min = 241.01KPa Max = 418.00KPa

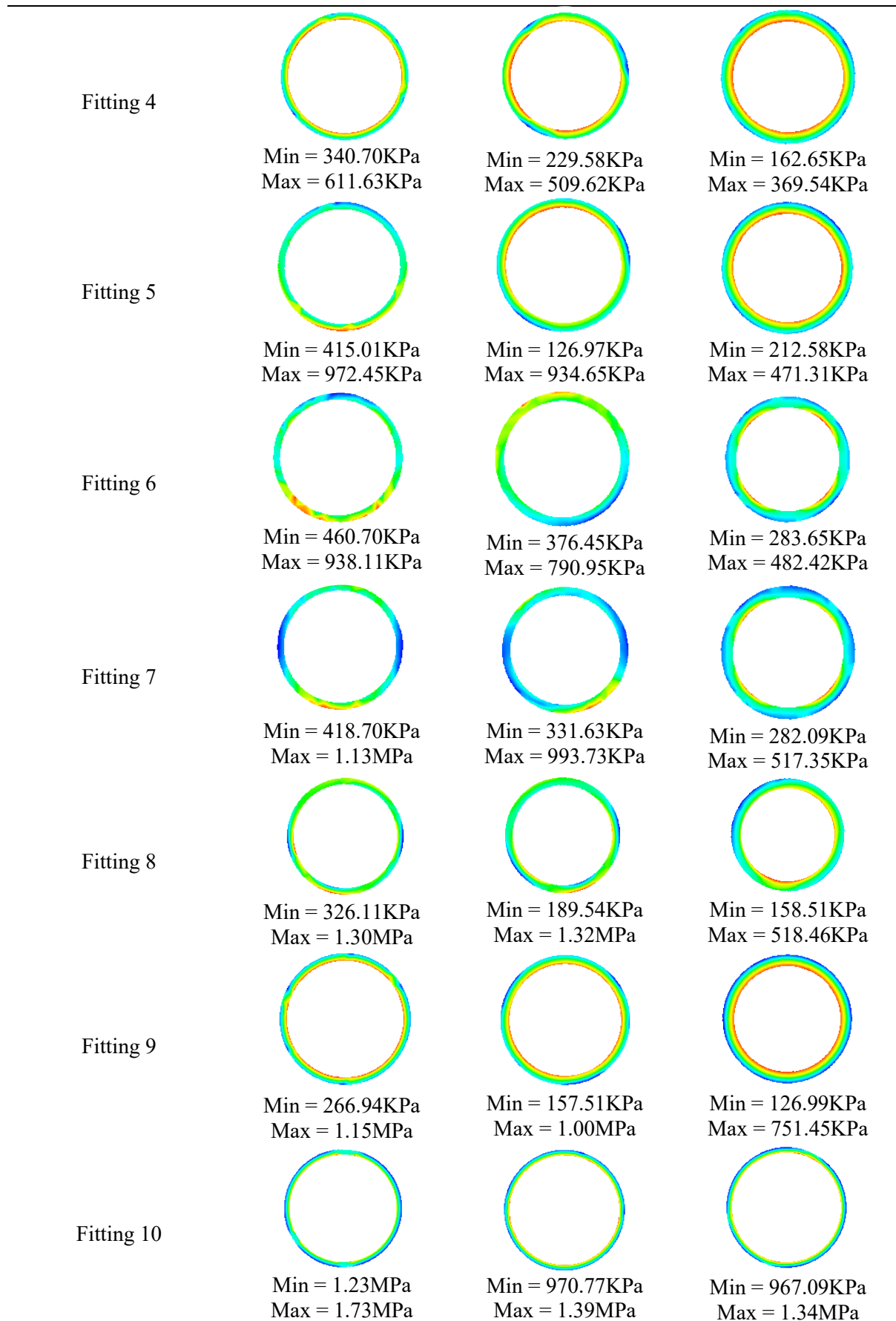
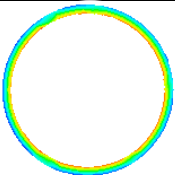
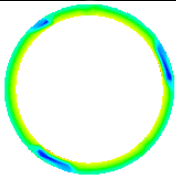
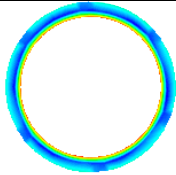
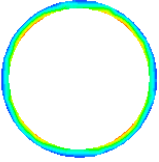
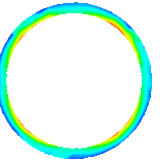
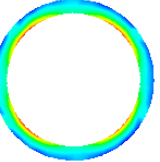
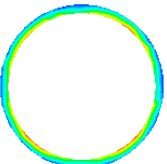
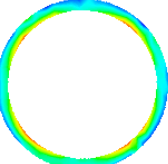

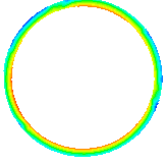
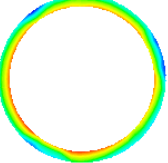

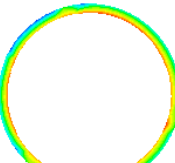
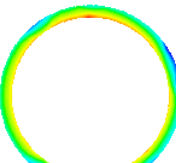

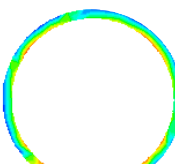
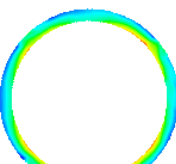

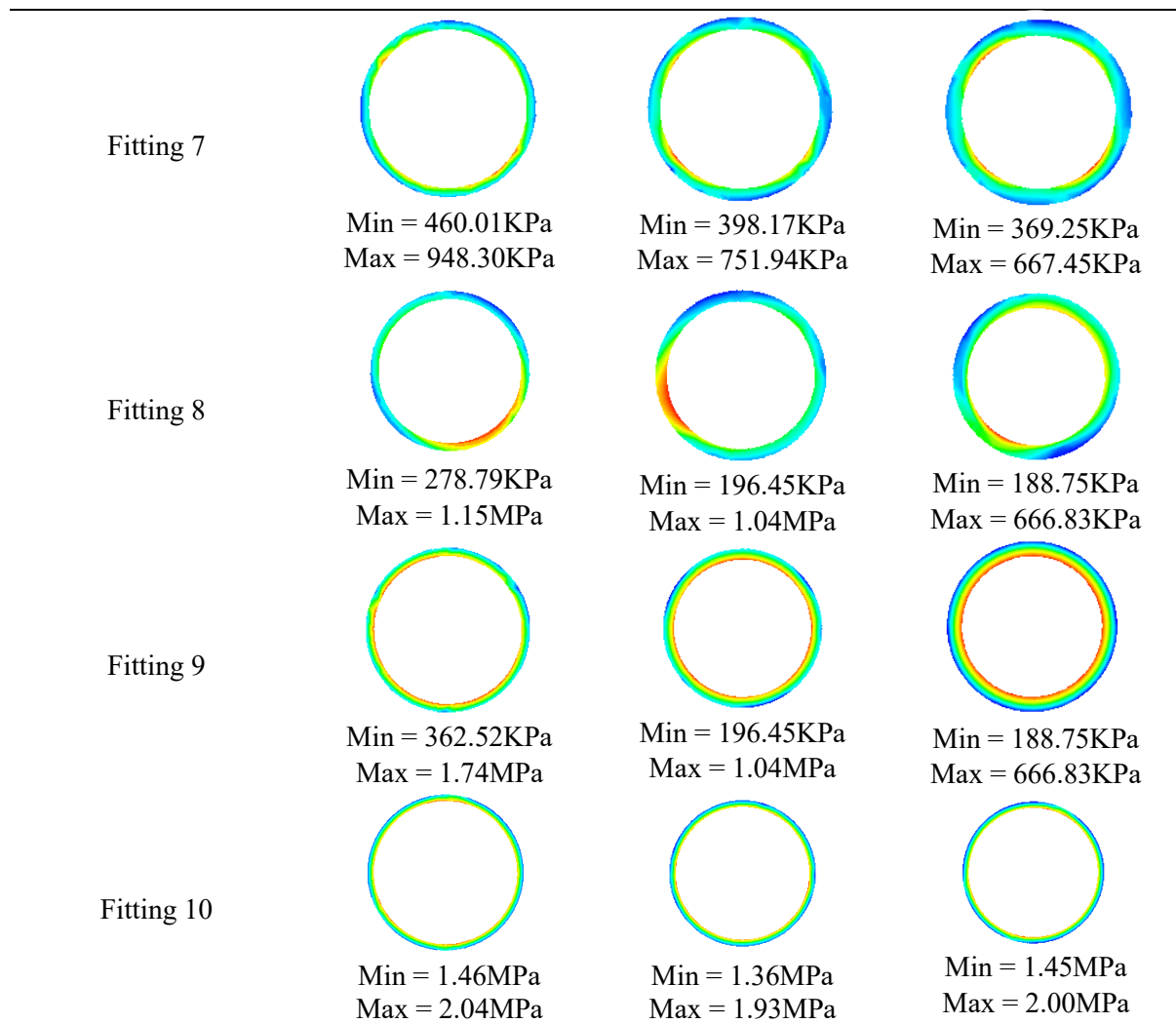


Table 2: Stress Distribution Along the Fitting at 250KPa Pressure Inlet

Risk	2.8mm	2.8mm	2.8mm
Fitting 1	 Min = 541.19KPa Max = 892.40KPa	 Min = 224.49KPa Max = 863.07KPa	 Min = 221.24KPa Max = 651.57KPa
Fitting 2	 Min = 385.23KPa Max = 653.81KPa	 Min = 314.27KPa Max = 541.08KPa	 Min = 253.19KPa Max = 441.06KPa
Fitting 3	 Min = 337.87KPa Max = 638.04KPa	 Min = 275.56KPa Max = 498.47KPa	 Min = 208.57KPa Max = 368.97KPa
Fitting 4	 Min = 285.44KPa Max = 551.95KPa	 Min = 188.74KPa Max = 472.17KPa	 Min = 121.81KPa Max = 315.61KPa
Fitting 5	 Min = 394.48KPa Max = 877.88KPa	 Min = 317.73KPa Max = 881.26KPa	 Min = 270.51KPa Max = 601.42KPa
Fitting 6	 Min = 485.98KPa Max = 876.85KPa	 Min = 435.27KPa Max = 780.20KPa	 Min = 353.02KPa Max = 610.84KPa



4. Conclusion

The objective of this study was to investigate the flow behavior effect from three different pipe wall thickness located at UTHM Biodiesel Pilot plant, to investigate the structural performance of the pipe effect from different pressure inlet and piping thickness to velocity and pressure distribution and lastly to construct the risk indicator to predict the risk for a new guideline of pipe lifespan in UTHM Biodiesel plant. Each model was analysed by using the Ansys Fluent and Ansys Mechanical to identify the flow and structure behavior. The Computational Fluid Dynamic (CFD) method was used to evaluate the velocity and pressure distribution as a flow behaviour of all models in the conclusion. The velocity distribution results showed that the velocity increased at the smaller section of the due to the area decrease and the fluid is forced to enter. In terms of pressure distribution, the pressure increased as soon as it entered the inlet and hit the bottom wall of the pipe. The greater the thickness of the wall, the greater the pressure drop, which reduces the velocity of the air to the pipe.

In this study, the Fluid-Structure Interaction (FSI) method was also used to evaluate the stress distribution on the three different pipe wall thickness models. According to the results, the pipe with 2.8mm has the highest stress distribution, particularly at 250.0 KPa pressure inlet as high as 4.8 MPa. At the end, risk indicator was established in order to make as a guideline to the lifespan of pipe in UTHM Biodiesel Pilot plant. As has been shown in both risk indicator result, the thickness of the pipe affected the flowrate and also the stress to the pipe wall. The higher the thickness of pipe wall, the lower the stress distribution. When pressure increase, the turbulent create inside the pipe increase.

Acknowledgement

The authors would like to thank Faculty of Engineering Technology, Universiti Tun Hussein Onn Malaysia for its support.

References

- [1] R. N. Rao, M. Maiya, S. Prabhu, G. Santhosh, and G. Hebbar, "The analysis of a piping system for improvement of a system in a process unit," *Mater. Today Proc.*, no. xxxx, 2021, doi: 10.1016/j.matpr.2021.02.595.
- [2] A. Bhatia, "Process Piping Fundamentals, Codes and Standards," no. 877, 2016, [Online]. Available: <https://www.cedengineering.com/userfiles/Process Piping Fundamentals, Codes and Standards - Module>
- [3] A. Iron, "Design Guidelines For Stainless Steel In Piping Systems A Designers ' Handbook Series."
- [4] C. M. B. Martins, J. L. Moreira, and J. I. Martins, "Corrosion in water supply pipe stainless steel 304 and a supply line of helium in stainless steel 316," *Eng. Fail. Anal.*, vol. 39, pp. 65–71, 2014, doi: 10.1016/j.engfailanal.2014.01.017.
- [5] A. Demirbas, "Importance of biodiesel as transportation fuel," *Energy Policy*, vol. 35, no. 9, pp. 4661–4670, 2007, doi: 10.1016/j.enpol.2007.04.003.
- [6] S. T. Keera, S. M. El Sabagh, and A. R. Taman, "Castor oil biodiesel production and optimization," *Egypt. J. Pet.*, vol. 27, no. 4, pp. 979–984, Dec. 2018, doi: 10.1016/j.ejpe.2018.02.007.
- [7] A. Demirbas, "Progress and recent trends in biodiesel fuels," *Energy Convers. Manag.*, vol. 50, no. 1, pp. 14–34, Jan. 2009, doi: 10.1016/j.enconman.2008.09.001.
- [8] S. P. Singh and D. Singh, "Biodiesel production through the use of different sources and characterization of oils and their esters as the substitute of diesel: A review," *Renewable and Sustainable Energy Reviews*, vol. 14, no. 1. Pergamon, pp. 200–216, Jan. 01, 2010, doi: 10.1016/j.rser.2009.07.017.
- [9] J. Tu, G.-H. Yeoh, and C. Liu, "CFD Mesh Generation: A Practical Guideline," in *Computational Fluid Dynamics*, Elsevier, 2018, pp. 125–154.
- [10] V. Bertram, "Introduction," in *Practical Ship Hydrodynamics*, Elsevier, 2012, pp. 1–39.
- [11] V. Hernandez-Perez, M. Abdulkadir, and B. J. Azzopardi, "Grid generation issues in the CFD modelling of two-phase flow in a pipe," *J. Comput. Multiph. Flows*, vol. 3, no. 1, pp. 13–26, 2011, doi: 10.1260/1757-482X.3.1.13.
- [12] M. Lee, G. Park, C. Park, and C. Kim, "Improvement of Grid Independence Test for Computational Fluid Dynamics Model of Building Based on Grid Resolution," *Adv. Civ. Eng.*, vol. 2020, 2020, doi: 10.1155/2020/8827936.
- [13] V. Demir, H. Yürdem, A. Yazgı, and T. Günhan, "Silindirik Tip Boru İçine Entegre Damlatıcılı Damla Sulama Borularında Farklı Boru Et Kalınlıklarının Damlatıcı Debileri Üzerine Etkisi," *Ege Üniversitesi Ziraat Fakültesi Derg.*, no. July, pp. 101–110, 2019, doi: 10.20289/zfdergi.485854.
- [14] A. O. Mohammed, H. H. Al-Kayiem, A. B. Osman, and O. Sabir, "One-way coupled fluid–structure interaction of gas–liquid slug flow in a horizontal pipe: Experiments and simulations," *J. Fluids Struct.*, vol. 97, p. 103083, 2020, doi: 10.1016/j.jfluidstructs.2020.103083.
- [15] J. C. Shieh, "FUNDAMENTALS OF Chapter 8 Pipe Flow," 2007.

- [16] I. Bjorklund, "Structural design of pressure pipes," *Water Sci. Technol. Water Supply*, vol. 1, no. 3, pp. 107–115, 2001, doi: 10.2166/ws.2001.0058.